Accuracy Assessment of Direct Georeferencing Using UAV Matrice 210 RTK V2 on Gully Santiš, Island of Pag (Croatia)

Katarina Glavačević[1], Ivan Marić[2] and Ante Šiljeg[2]
[1]*Independent Researcher, Ludwigshafen am Rhein, Germany*
[2]*Department of Geography, University of Zadar, Zadar, Croatia*

Keywords: Direct Georeferencing, Matrice 210 RTK V2, Absolute Accuracy, D-RTK 2, UAV Photogrammetry.

Abstract: Rapid development and increased availability of unmanned aerial vehicles (UAVs) resulted in the exponential use of these systems in many scientific fields and activities. However, the application of photogrammetric models derived using the Structure from Motion (SfM) technique largely depends on the use of ground control points (GCPs). Since the acquisition of the GCPs requires the use of high-quality total stations or GNSS-RTK receivers, these procedures generally take up a lot of time. Execution of a photogrammetric process without using the GCPs is called direct georeferencing, and it is becoming an increasingly popular method. In this research, we tested three methods of RTK positioning using the system of the *Matrice 210 RTK V2* and *D-RTK 2* mobile station. The following methods were tested: (a) D-RTK 2 as a base station; (b) D-RTK 2 correction with the third-party base station; (c) network NTRIP corrections CROPOS. An absolute accuracy assessment of each RTK positioning mode was done using 10 check points (CPs). By calculating the total RMSE, it was determined that (b) and (c) RTK positioning modes have a centimeter level of accuracy (<10 cm). In this research, it is determined that the tested UAV system for direct georeferencing can be used in a wide range of geographical applications and other disciplines where absolute accuracy of centimeter-level is required.

1 INTRODUCTION

The knowledge of accurate information about the Earth's surface has always played a key role in the development of scientific disciplines and activities (Guptill and Morrison, 1995, Šiljeg et al., 2018). Obtaining reliable spatial data is primarily based on the development of modern geospatial technologies (GST) (Linder, 2009). Accurate, precise, and fast collection of topographic data is becoming the basis of physical geography (Smith et al., 2016), other sciences, and sub-disciplines (Pike et al., 2009). Aerial, UAV and terrestrial photogrammetry is becoming a dominant technology in the study of various spatio-temporal changes. In recent years, obtaining high-resolution topographic models has been based on the application of UAV photogrammetry (Stott et al., 2020) and the SfM technique, which significantly accelerated the photogrammetric process (Masiero et al., 2017). The fundamental task of all photogrammetric techniques is to derive the geometric features of a certain object or scene (Dittrich et al., 2017). However, the dominance of UAV/SfM photogrammetry is limited by the need to mark and collect ground control points (GCPs) and check points (CPs) using quality and expensive GNSS receivers (Carbonneau and Dietrich, 2016). The GCPs and CPs need to be marked and measured according to the optimal distribution, which can be an extremely long and expensive process (Sanz-Ablanedo et al., 2018). It is generally considered that increasing the number of GCPs results in better model accuracy (Oniga et al., 2018). In the context of spatio-temporal analysis, additional problems arise due to the fact that GCPs can move or disappear due to surface deformations or weather conditions. Ultimately, a major limitation of this classic aerial photogrammetry approach is that sometimes it is not possible to achieve optimal GCPs and CPs distribution due to security or practical reasons (e.g. landslides, flood, frozen or swampy areas, etc.) (Zhang et al., 2019), the unavailability of the GNSS receiver, high energy relief, shortage of time, etc. Although the „classical“ way of performing aerial photogrammetry is recognized as the most important data collection method in the creation of topographic maps, it has obvious disadvantages in long production time, inefficiency, and dependence

Glavačević, K., Marić, I. and Šiljeg, A.
Accuracy Assessment of Direct Georeferencing Using UAV Matrice 210 RTK V2 on Gully Santiš, Island of Pag (Croatia).
In *Proceedings of the 9th International Conference on Geographical Information Systems Theory, Applications and Management (GISTAM 2023)*, pages 184-191
ISBN: 978-989-758-649-1; ISSN: 2184-500X

on GCPs, etc. (Yuan and Zhang, 2008). A new acceleration of the photogrammetric process comes with the appearance of the direct georeferencing (DG) method (Bláha et al., 2011, Rehak et al., 2013). The DG method does not require GCPs acquisition and aerotriangulation (AT) in the process of model derivation (Rizaldy and Firadus, 2012). DG represents a photogrammetric process in which modeling is based on the direct measurement of six exterior orientation (EO) parameters, that is, the position (XYZ) of the camera, which is measured by the GNSS receiver, and the orientation/inclination of the camera (pitch, roll, and yaw), which is measured by the inertial measurement unit (IMU), in real-time (Rizaldy and Firadus, 2012). However, the absence of GCPs represents a significant challenge in assessing the model's quality. The development of more affordable UAV platforms capable of producing models using the DG approach has begun in recent years. Therefore, the research about accuracy and suitability of such an approach as a full-fledged topographic imaging method is currently increasing (Liu et al., 2022, Zeybek, 2021, Carbonneau and Dietrich, 2016). Therefore, this research examines the accuracy of the DG approach using the popular UAV (Matrice 210 RTK V2 and D-RTK2) platform. The camera Zenmuse X7 DL-S 16mm F2.8 was used. The main goal of the research was to assess the accuracy of the DG method using the different modes of RTK positioning: (a) D-RTK 2 as a base station; (a_1) D-RTK 2 as a base station with the addition of a few GCPs; (b) D-RTK 2 correction with the third-party base station STONEX S10; (c) Network NTRIP corrections CROPOS.

Also, the following scenarios were tested:

(d) a classical photogrammetric approach using GCP and CP; (e) method using embedded navigation sensors (GPS/GNSS and IMU-MEMS) in UAVs.

The purpose of the research was to provide guidelines for the use of this setup at various scale (resolution). In this case study, the testing was not performed under the best possible conditions, because such conditions, especially in the case where the application of direct georeferencing is required, are not always possible. Therefore, the goal was to determine whether this sensor system corresponds to the manufacturer's claims in conditions (light wind, vertically dissected terrain) that are not ideal.

1.1 Gully Santiš (Pag Island)

The research area is gully Santiš (1163 m²), located on the southeastern coast of the Island of Pag (Croatia) (Figure 1). The island is dominated by Cretaceous-Paleogene carbonate deposits of limestone and dolomite, smaller parts of Paleogene flysch, and younger Quaternary deposits (Magaš, 2011). The gully was formed on accumulated thick brown soil, the deposits of which are prone to surface loss of material. The dimensions of the gully Santiš are 80 x 15 m, with an area of 1163 m^2, and a drainage basin with an area of 0.18 km^2 (Šiljeg et al. 2021).

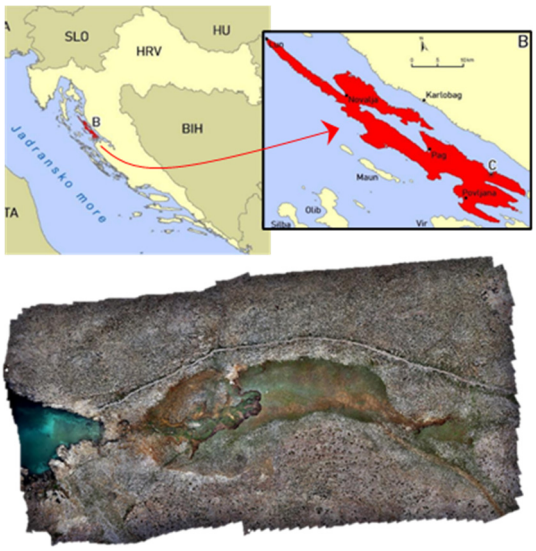

Figure 1: Location of gully Santiš in Croatia, Pag.

2 MATERIALS AND METHODS

The research methodology is divided into three main steps that include: (A) marking and measurement of ground control and check points (GCPs and CPs) within the research area; (B) derivation of digital surface models (DSM) and digital orthophoto (DOP) using: (b_1) classical photogrammetric image workflow process (with GCPs and CPs) and (b_2) through different ways of RTK positioning (1 - D-RTK2 as base station; 2 - D-RTK2 correction with a third party base station; 3- network NTRIP correction with CROPOS); (C) accuracy assessment of the derived models.

2.1 Connection of the UAV System

The D-RTK 2 mobile station was placed on an open, elevated area and was stabilized by a tripod using the built-in level. Open space means an environment without obstacles within a >200 m from the source of high-power radio emissions. After installation D-RTK 2 was not moved. The mobile station was turned on, and a constant green light on the *power* indicator

indicated that D-RTK2 was connected to ≥10 satellites. Then the (4th) operating mode was selected, which is intended for work with Matrice 210 RTK V2. Successful connection is done if the orientation and positioning status of the is in FIX mode. The UAV takeoff location had to be visible from the base station location. The selected location in the middle of the gully was visible from the D-RTK2 mobile station. UAV mission planning was done in the DJI Pilot application, single-grid missions were planned with a front and side photo overlap of 80%. The flight height was set at 30 m. The flight speed in the mission was 2 m/s.

2.1.1 D-RTK 2 as Base Station

The first tested method of RTK positioning was the D-RTK2 as base station. This method uses only the D-RTK2 base station to transmit RTK information directly to the UAV (Fig. 2). The base station is turned on and it connects to the controller and the UAV. The primary benefit of this method is very easy set up. This workflow does not require an internet connection. If the default coordinates measured with D-RTR2 are used in the Z value, the height of the base station does not have to be added. The D-RTK2 measures long. and lat. in decimal degrees (DD), and altitude as height above ellipsoidal height (HAE[1]).

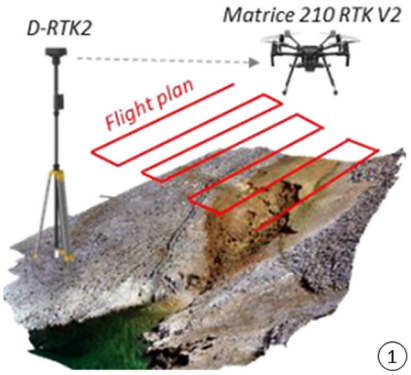

Figure 2: D-RTK2 as a base station.

2.1.2 D-RTK 2 Coordinate Correction with a Stonex S10

In the second method of RTK positioning, the precise determination of the D-RTK2 coordinates was performed by using the STONEX S10 GNSS receiver, which was mounted using a suitable tripod on the same location as D-RTK2 (Fig. 3).

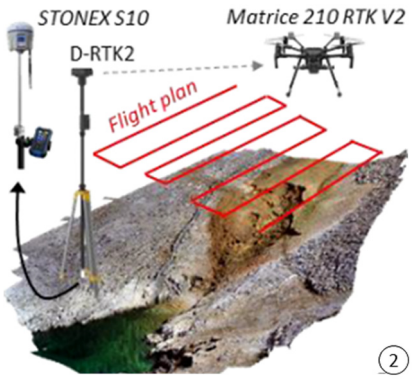

Figure 3: D-RTK2 coordinate correction with a STONEX S10.

After the initialization of the receiver, the measurement of the point where the D-RTK2 was mounted lasted 2 min (10 measurement epochs). The measured coordinates, using STONEX S10 and NRTK modality, were entered in the DJI GO application. The precision of the measurement was in accordance with the official specifications of the STONEX S10. Since there is no place in the application to enter the height of the base station, the measured coordinates representing the antenna phase center (APC) of the D-RTK2 were entered (1.802 m) (Buonanno, 2019). The height of the antenna is calculated as follows: the tripod provided by DJI has a height of 1,660 m from the end to the bottom of the antenna. Adding the distance between the base of the antenna and the phase center of the antenna (0.1419 m) gives a value of 1.802 m, which is added to the reference height in the DJI GS RTK settings. In summary, the measured coordinates representing the phase center of the antenna (APC) D-RTK 2 are entered. Table 1 shows the differences in the coordinates of the location where the D-RTK 2 mobile station was mounted, measured by the STONEX S10 and the D-RTK2 mobile station. The D-RTK2 measured the height of the antenna almost 40 cm lower. The differences for longitude are about 73.3 cm and for latitude 43.9 cm. Therefore, the assumption was that the model generated by RTK positioning using the first operating mode, i.e. where only D-RTK2 is used as a base station, will deviate from the model derived by the classic approach in similar values (long. ≈ 73.3 cm, lat. ≈ -43.869 cm, elev. ≈ 38,60 cm).

[1] Height Above Ellipsoid

Table 1: Differences in base station coordinates measured with D-RTK2 (mode 1) and Stonex S10 (mode 2).

WGS84	X (dd)	Y (dd)	Z (m)
D-RTK2	15.19281974	44.37452990	69.331
Stonex S10	15.19281054	44.37453387	69.717
Diff. (cm)	**73.366**	**-43.869**	**-38.60**

2.1.3 Network NTRIP Correction with CROPOS

In the third method of RTK positioning, the Networked Transport of RTCM via the Internet Protocol (NTRIP) connection option was used (Fig. 4). This methodology uses NTRIP without a base station of any kind and provides live RTK data using an NTRIP stream connected to the Internet. This process requires an internet connection at the recording location via local Wi-Fi, hotspot, or dedicated 5G connection to the controller. The advantage of this method is that using a networked workflow requires the least amount of physical equipment at the recording location. The biggest disadvantage is the need for an active, reliable internet connection. Even a brief interruption of the Internet connection can cause problems.

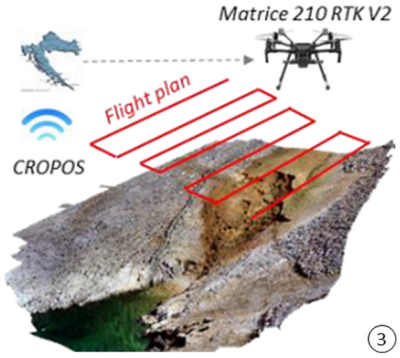

Figure 4: Network NTRIP correction with CROPOS.

2.2 Marking and Acquisition of GCPs and CPs

The arrangement of GCPs/CP was determined by the type of shallow brown soil, extremely dynamic and subject to erosion that prevails in the research area. Furthermore, certain parts of the gully are extremely vertically dissected with a large slope, which complicates the process of marking and acquisition of GCPs and CPs. The majority of points were marked on limited rocky surfaces, which are characterized by small surface slopes. A total of 10 points were marked and collected in the research area in order to verify the accuracy of the derived models. The coordinates were collected using a STONEX S10 GNSS receiver which in RTK mode has a horizontal accuracy of 0.8 cm and a vertical accuracy of 1.5 cm. After the initialization, the points were measured in one independent measurement, and each point was measured for 2 min (10 measurement epochs) (Fig. 5). The coordinates of the marked points were collected in the WGS84 coordinate system in decimal degrees (DD), while the altitude was collected as ellipsoidal height (HAE).

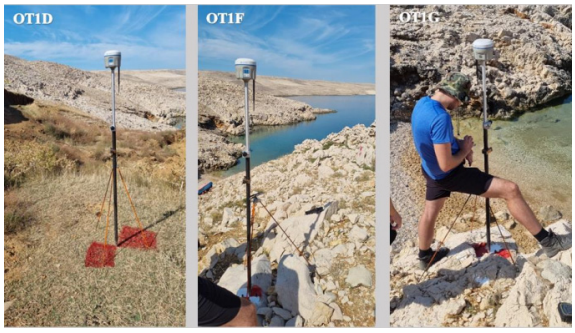

Figure 5: Acquisition of GCPs and CPs.

2.3 Processing of UAV Images

In each mission about 240 images were collected. Flight time of each mission was 14 minutes. UAV images were processed using Agisoft Metashape 1.5.1. software. The process consisted of seven commonly known steps in the SfM photogrammetry process (Marić et al., 2019): (1) image quality checking; (2) camera accuracy settings; (3) align photos; (4) gradual selection and optimization of the camera position; (5) adding GCPs and/or; (6) build a dense cloud, mesh, and texture; (7) build and export digital surface model (DSM), and digital orthophoto (DOP). The quality of all photos was assessed. Those photos with a quality value < 0.5 were deleted. In the first step (align photos) about 20 million tie points were generated. The *accuracy* parameter in *align photos* is set to high, and the key point limit and ie point limit are set to 40000 and 8000. Interior camera calibration parameters were determined automatically after alignment. Using the gradual selection, all tie points with reprojection error greater than 0.2 and reconstruction uncertainty greater than 20 were deleted. The GCPs and CPs were added to the reconstructed sparse point cloud. In some models, all points served as GCPs, while in others, all points served as CPs. In cases where GCPs/ CPs were added, and the reconstructed model was updated, it was observed that certain camera locations (photos) have a significant positioning error (e.g. >40 cm). Therefore, a smaller number of these photos were

deleted, which were mostly located at the edges of the mission. This process decreased the model error. DSM and DOP were derived from the point cloud, which had approximately 101 million points (Fig. 6).

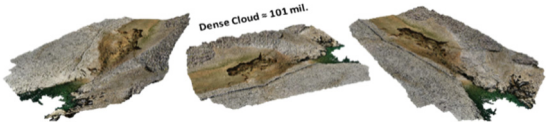

Figure 6: Derived dense point cloud.

3 RESULTS

3.1 GCP and Check Points

All points were collected using GNSS Stonex S10 and NRTK modality, and the precision of the measurement was calculated from 10 measurements collected at each point. Table 2 shows the mean range value for XYZ coordinates. The precision of the collected points corresponds to the specified factory precision of the receiver. The X coordinate deviates on average by 0.83 cm, the Y coordinate the same, and the Z coordinate slightly higher (Table 2).

Table 2: The average range of XYZ coordinate values.

	Range (cm)		
GCP/CP	**X**	**Y**	**Z**
A	0.61	0.69	0.90
B	0.73	0.77	1.80
D	0.37	0.80	0.7
E	0.90	1.06	1.00
F	1.18	0.80	0.90
G	0.71	0.88	1.2
H	1.13	0.74	1.30
I	1.01	0.91	0.50
J	0.97	0.91	1.00
K	0.72	0.70	0.70
MEAN	**0.83**	**0.83**	**1.00**

3.2 The Classical Photogrammetric Methods

The classic method refers to the dominant way of performing the UAV photogrammetry process (Fig. 7). In this image processing workflow, the D-RTK 2 mobile station was not used. The collected GCPs (n=6) were used to position the reconstructed model in a global coordinate system, while the CPs (n=4) were used to check the accuracy of the model.

The recorded surface area was 0.0143 km². The ground samplig distance (GSD) of the DOP was 6.62 mm, and the DSM was 1.32 cm. Point density was 5700 points/m². From the added CPs the root mean square error (RMSE) was calculated. The RMSE for the X coordinate was 1.33 cm, for the Y 1.28 cm, and for the Z 2.76 cm. The total RMSE of this model was 3.32 cm.

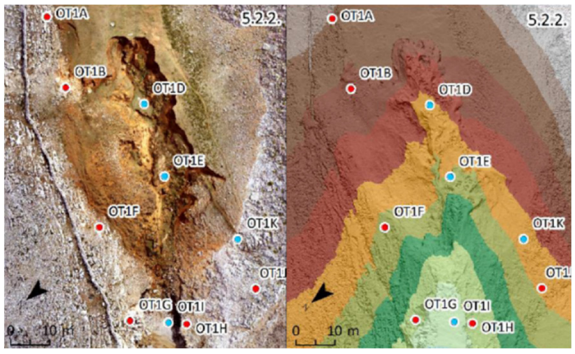

Figure 7: Derived DOP and DSM (classical method).

3.3 Direct Georeferencing

3.3.1 D-RTK 2 as Base Station

In this method of RTK positioning the D-RTK 2 mobile station was used. All collected points were used as CP (n=10) (Fig. 8). The RMSE for the X coordinate was 75.89 cm, for the Y 34.98 cm, and for the Z 26.94 cm. The total RMSE was 87.80 cm. The large total RMSE is not surprising the difference in the coordinates of the mobile station location measured by D-RTK 2 itself and those by Stonex S10 is known (Table 1). The total RMSE was extremely large (87.809 cm) due to the incorrect measurement of the location of D-RTK 2. In this reconstructed model, a smaller number of GCPs were added, with the aim of determining their impact on model accuracy. An iterative assessment of the accuracy of the model was performed (Table 3), first with one, then two, and finally with three GCP added. Thus, in the 1_{st} scenario, nine CPs were used, in the 2_{nd} eight, and in the 3_{rd} seven CPs.

Table 3: The accuracy of different scenarios (D-RTK + GCPs).

	X error (cm)	**Y error (cm)**	**Z error (cm)**	**Total (cm)**
D-RTK2 **+1GCP**	20.37	11.68	31.99	**39.68**
D-RTK2 **+2GCP**	21.57	9.36	23.05	**32.93**
D-RTK2 **+3GCP**	15.10	7.36	9.08	**19.09**

It can be seen that the total RMSE decreases with the addition of GCPs. By adding just one GCP, the total RMSE decreased by 48.129 cm. The second GCP reduced the RMSE by 6.75 cm, and the third by

13.84 cm. The total RMSE was reduced by 68.719 cm by adding only three GCPs.

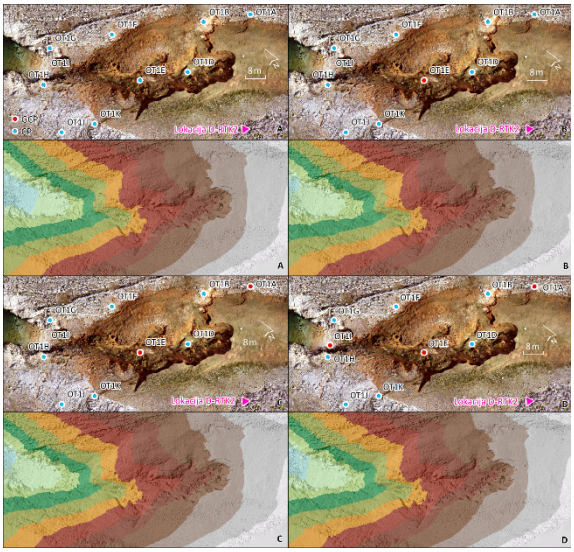

Figure 8: Derived DOPs and DSMs. (A) D-RTK; (B) D-RTK+1GCP; (C) D-RTK+2GCP; (D) D-RTK+3GCP.

3.3.2 D-RTK 2 Coordinate Correction with STONEX S10

In this method of RTK positioning a GNSS receiver, Stonex S10 was used in measuring the exact coordinates of the location of the D-RTK 2 mobile station. As in the first scenario on all acquired points were used as CPs (n=10). The RMSE for the X coordinate was 4.09 cm, for the Y 2.69 cm, and for the Z 5.97 cm. The total RMSE of this model was 7.72 cm. The points "OT1A" and "OT1B", which were located on the least number of photos, had the highest total RMSE. If these two points were excluded from the analysis, the total RMSE of the model derived by RTK positioning using the Stonex S10 correction would amount to 5.99 cm.

3.3.3 Network NTRIP Corrections with CROPOS

In this method of RTK positioning the NTRIP connection option with CROPOS (*Croatian Positioning System*) was used, providing real-time RTK data without a base station on the site. All collected points were used as CPs (n=10) (Fig. 9). The RMSE for the X coordinate was 4.044 cm, for the Y 2.228 cm, and for the Z 4.488 cm. The total RMSE of this model is 6.44 cm. The points "OT1A" and "OT1B", which were located on the least number of photos (15 and 25), had the highest total RMSE. If these two points were excluded from the analysis, the total RMSE of the model derived from RTK positioning using the network NTRIP correction would be 5.31 cm.

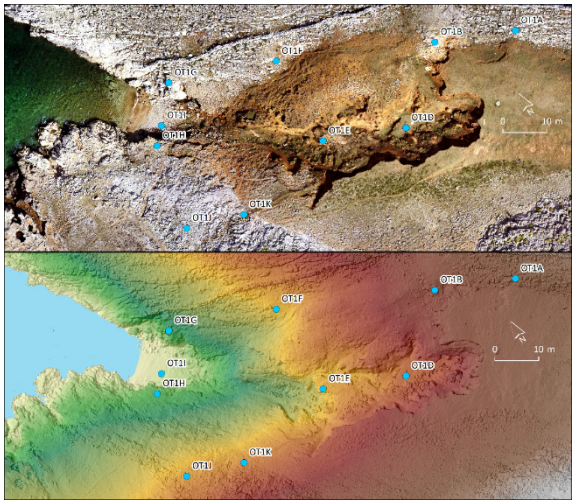

Figure 9: Derived DOP and DSM (NTRIP connection with CROPOS).

3.4 Absolute Accuracy of Tested RTK Positioning Modes

The official specifications that can be found for many sensor systems are usually tested and determined under best-case scenarios. In this case, the testing was not performed under best-case scenarios precisely because such conditions, especially in the case where the application of direct georeferencing is required, are not always possible. In general, the goal was to determine if this sensor system corresponds to the manufacturer's own claims in conditions that are not ideal. It was found that the accuracy of direct georeferencing using the Matrice 210 RTK V2 and the D-RTK 2 depends on the selected mode of operation. Three modes of RTK positioning were tested. Table 4 shows the summary results of XYZ and total RMSE for the derived models. The highest accuracy, as expected, was achieved in scenario (d) with the application of GCP and CP resulting in a total RMSE of 3.22 cm. Furthermore, the centimeter level of accuracy (<10 cm) was achieved in the operating mode where the (c) NTRIP connection option with CROPOS was used, which enables the positioning of the UAV in real-time, and in the operating mode where the (b) corrective coordinates collected by the Stonex S10 receiver were used (Table 4). These two methods give similar results, which is expected considering that the STONEX S10 uses the CROPOS system of base stations. The

advantage of the first method is, that using a network NTRIP connection option, requires the least amount of equipment at the recording location. The biggest disadvantage is the need for an active, reliable Internet connection. In the second method, another high-precision GNSS receiver is needed, which could measure the coordinate on which the D-RTK 2 mobile station was mounted.

Table 4: Summary data on the accuracy of all tested RTK positioning methods.

Scenario	X error (cm)	Y error (cm)	Z error (cm)	Total (cm)
D	1.33	1.28	2.76	3.32
C	4.04	2.23	4.49	6.44
B	4.06	2.69	5.97	7.72
A1 +3GCP	15.10	7.36	9.08	19.09
A1 +2 GCP	21.57	9.36	23.05	32.93
A1 +1 GCP	20.37	11.68	31.99	39.68
A	75.90	34.98	26.94	87.81
E	75.48	70.78	93.78	139.7

(a) D-RTK 2 as a base station; (a_1) D-RTK 2 with the addition of few GCPs; (b) D-RTK 2 correction with the Stonex S10; (c) network NTRIP corrections CROPOS; (d) classical approach using GCP and CP; (e) method using embedded navigation sensors into UAVs.

The large total RMSE of 87.81 cm which is recorded for D-RTK 2 is not surprising considering the differences in the location coordinates of the mobile station measured by D-RTK 2 itself and those by STONEX S10 (Table 1). Therefore, the deviation in the location of D-RTK 2 contributed to this error (Table 4). Namely, in the official specifications, it is stated that the accuracy of RTK positioning is centimeters (horizontal = 1 cm, vertical = 2 cm). This means that, in ideal recording conditions (absence of wind), the relative accuracy of the positioning of the cameras (photos location) will be in centimeters. However, the single point (absolute) accuracy is 1.5 m horizontally and 3 m vertically. Therefore, this result is not surprising. By including a smaller number of GCPs (n=3) there is a significant reduction in model error (87.81 cm - 19.09 cm). However, the final total RMSE is still too large (19.09 cm) to justify the use of XYZ coordinates of the photos in model orientation. Based on this research, it can be concluded that, if the D-RTK 2 mobile station retains this level of absolute accuracy in reading its own location (≈ 1 m), it is not worth using a smaller number of GCPs in the orientation of the model, because ultimately, in order to obtain satisfactory accuracy, a larger number of them should be added (> 3), which would make the very application of D-RTK 2 senseless if it is about the smaller surface. In scenario (E), the D-RTK 2 mobile station was not used for positioning, and GCPs were not used in the photogrammetric process. The RTK positioning mode was turned off, and only the XYZ coordinates of the photos from the UAV's GNSS receiver were used. In this case, all 10 points were used to check the accuracy of the model (CP=10). The RMSE for the X coordinate was 75.5 cm, for the Y 70.8 cm, and for the Z 93.8 cm. The total RMSE of this model was 139.7 cm. Nevertheless, the accuracy of positioning is satisfactory considering that only XYZ data of the photos, collected with the UAV's GNSS receiver, were used in the process of model orientation.

4 CONCLUSIONS

The research tested three modes of RTK positioning using the Matrice 210 RTK V2 system and D-RTK 2 mobile station. An assessment of the absolute accuracy of the photogrammetric models was carried out through the marking and collection of GCPs/ CPs (n=10).

By calculating the total RMSE, it was determined that two (NTRIP network correction with CROPOS and STONEX S10 correction) of the three tested RTK positioning modes have a centimeter level of accuracy. It was found that the accuracy of RTK positioning using the Matrice 210 RTK V2 and the D-RTK 2 mobile station depends on the selected mode of operation. These two methods give similar results, which is expected given that the STONEX S10 uses the CROPOS system of base stations. The third method of RTK positioning, where the D-RTK determines its location by itself, generates a large absolute error. This error is not surprising, considering the differences in the location coordinates of the mobile station read by D-RTK 2 itself and those read by STONEX S10. This research established that the tested UAV system for direct georeferencing can be used in a wide range of geographic sciences and other disciplines where absolute centimeter accuracy of different models is required.

ACKNOWLEDGEMENTS

This work has been supported in part by Croatian Science Foundation under the project UIP-2017-05-2694 and conducted within Center for Geospatial Technology.

REFERENCES

Bláha, M., Eisenbeiss, H., Grimm, D., & Limpach, P. (2011). Direct georeferencing of UAVs, In *Proceedings of the International Conference on Unmanned Aerial Vehicle in Geomatics* (UAV-g) (Vol. 38, pp. 131-136). Copernicus.

Buonanno, M. (2019): *D-RTK2 - User Notes - rev_200417*, CNR-ISAFOM, Italy.

Carbonneau, P. E., Dietrich, J. T. (2016): Cost-effective non-metric photogrammetry from consumer-grade sUAS: implications for direct georeferencing of structure from motion photogrammetry, *Earth Surface Processes and Landforms*, 42(3), 473-486.

Dittrich, A., Weinmann, M., Hinz, S. (2017): *Analytical and numerical investigations on the accuracy and robustness of geometric features extracted from 3D point cloud data.* ISPRS journal of photogrammetry and remote sensing, 126, 195-208.

Guptill, S. C., Morrison, J. L. (1995). Looking ahead. *In Elements of spatial data quality* (pp. 189-197). Pergamon

Linder, W. (2009). *Digital photogrammetry* (Vol. 1). Berlin: Springer.

Liu, X., Lian, X., Yang, W., Wang, F., Han, Y., Zhang, Y. (2022): Accuracy assessment of a UAV direct georeferencing method and impact of the configuration of ground control points. *Drones*, 6(2), 30.

Magaš, D. (2011). *Zemljopisna obilježja otoka Paga u funkciji upoznavanja njegove toponimije.* Toponimija otoka Paga, 5-49.

Marić, I., Šiljeg, A., Domazetović, F. (2019): Geoprostorne tehnologije u 3D dokumentaciji i promociji kulturne baštine–primjer utvrde Fortica na otoku Pagu. *Geodetski glasnik*, 50, 19-44.

Masiero, A., Fissore, F., Vettore, A. (2017). A low-cost UWB based solution for direct georeferencing UAV photogrammetry, *Remote Sensing*, 9(5), 414.

Oniga, V. E., Breaban, A. I., Statescu, F. (2018). *Determining the optimum number of ground control points for obtaining high precision results based on UAS images.* In Multidisciplinary Digital Publishing Institute Proceedings (Vol. 2, No. 7, p. 352).

Pike, R. J., Evans, I. S., Hengl, T. (2009). Geomorphometry: a brief guide. *Developments in Soil Science*, 33, 3-30.

Rehak, M., Mabillard, R., Skaloud, J. (2013): *A micro-UAV with the capability of direct georeferencing*, International Archives of the Photogrammetry, Remote Sensing and Spatial Information Sciences, Volume XL-1/W2, 4 – 6 September 2013, Rostock, Germany.

Rizaldy, A., Firdaus, W. (2012). *Direct georeferencing: A new standard in photogrammetry for high accuracy mapping,* International Archives of the Photogrammetry, Remote Sensing and Spatial Information Sciences, Volume XXXIX-B1, XXII ISPRS Congress, 25 August – 01 September 2012, Melbourne, Australia

Sanz-Ablanedo, E., Chandler, J. H., Rodríguez-Pérez, J. R., Ordóñez, C. (2018): Accuracy of unmanned aerial vehicle (UAV) and SfM photogrammetry survey as a function of the number and location of ground control points used, *Remote Sensing*, 10(10), 1606.

Šiljeg, A., Barada, M., Marić, I. (2018): *Digitalno modeliranje reljefa*, Alfa d.d., Sveučilište u Zadru, Zadar.

Šiljeg, A., Domazetović, F., Marić, I., Lončar, N., Panđa, L. (2021). *New Method for Automated Quantification of Vertical Spatio-Temporal Changes within Gully Cross-Sections Based on Very-High-Resolution Models.* Remote Sensing, 13(2), 321.

Smith, M. W., J. L. Carrivick, D. J. Quincey (2016): *"Structure from motion photogrammetry in physical geography."* Progress in Physical Geography 40.2 247-275.

Stott, E., Williams, R. D., Hoey, T. B. (2020): Ground control point distribution for accurate kilometre-scale topographic mapping using an RTK-GNSS unmanned aerial vehicle and SfM photogrammetry. *Drones*, 4(3), 55.

Yuan, X., Zhang, X. P. (2008): Theoretical accuracy of direct georeferencing with position and orientation system in aerial photogrammetry. *The International Archives of the Photogrammetry, Remote Sensing and Spatial Sciences*, 617-622.

Zeybek, M. (2021). Accuracy assessment of direct georeferencing UAV images with onboard global navigation satellite system and comparison of CORS/RTK surveying methods. *Measurement Science and Technology*, 32(6), 065402.

Zhang, H., Aldana-Jague, E., Clapuyt, F., Wilken, F., Vanacker, V., Van Oost, K. (2019): Evaluating the Potential of PPK Direct Georeferencing for UAV-SfM Photogrammetry and Precise Topographic Mapping. *Earth Surf. Dyn. Discuss*, 1-34.